The Journal of Pathology: Clinical Research
J Pathol Clin Res September 2021; **7:** 446–458
Published online 12 May 2021 in Wiley Online Library (wileyonlinelibrary.com). DOI: 10.1002/cjp2.224

ORIGINAL ARTICLE

Dysbalance of ACE2 levels – a possible cause for severe COVID-19 outcome in COPD

Elisabeth Fließer[1†], Anna Birnhuber[1†], Leigh M Marsh[1], Elisabeth Gschwandtner[2], Walter Klepetko[2], Horst Olschewski[3] and Grazyna Kwapiszewska[1,4*]

[1]*Ludwig Boltzmann Institute for Lung Vascular Research, Graz, Austria*
[2]*Division of Thoracic Surgery, Department of Surgery, Medical University of Vienna, Vienna, Austria*
[3]*Division of Pulmonology, Medical University of Graz, Graz, Austria*
[4]*Otto Loewi Research Center, Medical University of Graz, Graz, Austria*

**Correspondence to: Grazyna Kwapiszewska, Ludwig Boltzmann Institute for Lung Vascular Research, Neue Stiftingtalstraße 6/VI, 8010 Graz, Austria. E-mail: grazyna.kwapiszewska@lvr.lbg.ac.at*

†These authors contributed equally to this study.

Abstract

Severe acute respiratory syndrome coronavirus 2 (SARS-CoV-2) poses a serious threat to healthcare systems worldwide. Binding of the virus to angiotensin-converting enzyme 2 (ACE2) is an important step in the infection mechanism. However, it is unknown if ACE2 expression in patients with chronic lung diseases (CLDs), such as chronic obstructive pulmonary disease (COPD), idiopathic pulmonary arterial hypertension (IPAH), or pulmonary fibrosis (PF), is changed as compared to controls. We used lung samples from patients with COPD ($n = 28$), IPAH ($n = 10$), and PF ($n = 10$) as well as healthy control donor ($n = 10$) tissue samples to investigate the expression of ACE2 and related cofactors that might influence the course of SARS-CoV-2 infection. Expression levels of the *ACE2* receptor, the putative receptor CD147/*BSG*, and the viral entry cofactors *TMPRSS2* (transmembrane serine protease 2), *EZR*, and *FURIN* were determined by quantitative PCR and in open-access RNA sequencing datasets. Immunohistochemical and single-cell RNA sequencing (scRNAseq) analyses were used for localization and coexpression, respectively. Soluble ACE2 (sACE2) plasma levels were analyzed by enzyme-linked immunosorbent assay. In COPD as compared to donor, IPAH, and PF lung tissue, gene expression of *ACE2*, *TMPRSS2*, and *EZR* was significantly elevated, but circulating sACE2 levels were significantly reduced in COPD and PF plasma compared to healthy control and IPAH plasma samples. Lung tissue expressions of *FURIN* and CD147/*BSG* were downregulated in COPD. None of these changes were associated with changes in pulmonary hemodynamics. Histological analysis revealed coexpression of ACE2, TMPRSS2, and Ezrin in bronchial regions and epithelial cells. This was confirmed by scRNAseq analysis. There were no significant expression changes of the analyzed molecules in the lung tissue of IPAH and idiopathic PF as compared to control. In conclusion, we reveal increased ACE2 and TMPRSS2 expression in lung tissue with a concomitant decrease of protective sACE2 in COPD patients. These changes represent the possible risk factors for an increased susceptibility of COPD patients to SARS-CoV-2 infection.

Keywords: chronic obstructive pulmonary disease; COPD; chronic lung disease; COVID-19; SARS-CoV-2; ACE2; TMPRSS2; pulmonary fibrosis; pulmonary hypertension

Received 15 February 2021; Revised 22 March 2021; Accepted 21 April 2021

Conflict of interest statement: HO reports personal fees and nonfinancial support from Bayer, Pfizer, Novartis, and Boehringer; grants, personal fees, and nonfinancial support from Actelion; grants and personal fees from MSD; grants from Inventiva and Algorithm Sciences; and personal fees from Chiesi, Menarini, MedUpdate, Astra Zeneca, and GSK, outside the submitted work. The other authors declare no conflicts of interest.

Introduction

Severe acute respiratory syndrome coronavirus 2 (SARS-CoV-2) causes acute respiratory tract infections, termed COVID-19, and leads to heterogeneous clinical manifestations of variable severity [1]. There is evidence that patients with chronic lung diseases (CLDs), such as chronic obstructive pulmonary disease (COPD), develop severe illness more frequently [2–4]. However, the underlying reasons and the

contribution of pulmonary hypertension, a common complication in CLD patients, have remained elusive.

Similar to the prior coronavirus subtypes, SARS-CoV-1 and Middle East respiratory syndrome coronavirus, SARS-CoV-2 uses angiotensin-converting enzyme 2 (ACE2) as the main vehicle for cell entry [5,6]. In the lungs, the receptor is reportedly expressed on various cell types, including type I and type II alveolar cells, smooth muscle cells, or macrophages, whereas reports on its expression on endothelial cells are still controversial [7,8]. Alternatively, CD147 is debated as a putative host factor, interacting with SARS-CoV-2 [9,10]. In addition, specific host proteases, such as Furin and transmembrane serine protease 2 (TMPRSS2), are needed to process the virus surface spike (S)-protein in order for the virus to fuse with the host cell membrane after engaging ACE2 [5,11]. Once the virus has successfully infected an individual, the clinical symptoms and severity of the COVID-19 disease can be manifold. The most common symptoms are fever, cough, dyspnea, headache, and diarrhea [1]. The severity is very heterogeneous, ranging from no symptoms to severe acute respiratory distress syndrome [12]. In addition, cardiovascular complications and 'endothelialitis' have been described [13]. Patients with preexisting CLDs, affecting either the airways, the pulmonary parenchyma, or the vasculature, might therefore be at high risk of severe COVID-19 pneumonia.

Although more detailed evaluations show a lower prevalence of COVID-19 among asthma patients and do not suggest asthma as an individual risk factor for severe outcome, few studies have focused on the assessment of SARS-CoV-2-associated genes in CLD such as COPD, pulmonary fibrosis (PF), or idiopathic pulmonary arterial hypertension (IPAH) [14–18]. A detailed meta-analysis revealed COPD to be significantly associated with mechanical ventilation, intensive care unit (ICU) requirement, and death, although infection numbers are similar to the broad population [4]. Data on SARS-CoV-2 infections in IPAH patients are very limited, although early reports point toward an increased case fatality [19,20].

Here, our objective was to gain detailed insights into gene expression, localization, and shedding of SARS-CoV-2 relevant molecules ACE2, TMPRSS2, Furin, Ezrin (EZR), and CD147 (Basigin [BSG]) in the lung tissue and systemic circulation of COPD, IPAH, and PF as compared to controls. We also aimed to determine whether there is an association with pulmonary hemodynamics. By simultaneously analyzing this comprehensive set of costimulatory molecules as well as by correlating results with clinical parameters, we aimed to link molecular properties to susceptibility for severe COVID-19 pneumonia.

Materials and methods

Study population

Lung samples from patients with COPD ($n = 28$), IPAH ($n = 10$), and PF ($n = 10$) as well as control lung tissue from downsized donor lungs ($n = 10$) were collected between 2011 and 2016. Patient and donor lungs were achieved during lung transplantation (LTX) at the Department of Surgery, Division of Thoracic Surgery, Medical University of Vienna, Austria. The protocol and tissue usage were approved by the institutional ethics committee and patient consent was obtained before LTX. Patient characteristics included age at the time of LTX, body mass index (BMI), sex, smoking status, oxygen requirement, partial pressure of CO_2 (pCO_2), partial pressure of O_2 (pO_2), mean pulmonary arterial pressure (mPAP), and pulmonary function tests, and are presented in Tables 1 and 2. The study cohort was partially described in Refs [21–23]. Healthy control samples were prospectively collected and stored in the Biobank of the Medical University of Graz between 2011 and 2015. Written

Table 1. Demographics and clinical characteristics of COPD, IPAH, and PF patients and donors used for qPCR analysis.

	Donor	COPD	IPAH	PF
Subjects (*N*)	10	28	10	9
Sex (male:female)	4:6	13:16	3:7	6:3
Age at LTX (years)	41 ± 18.7	57 ± 5.6	31 ± 12.2	56 ± 9.2
BMI (kg/m^2)	25 ± 4.3	22 ± 2.5	20 ± 3.1	25 ± 4.2
Smoking status (never/former/active/unknown)	NA	1/23/0/5	NA	NA
FEV_1 (% predicted)	NA	23 ± 11.2	73 ± 7.0	43.3 ± 10.7
FVC (% predicted)	NA	48 ± 18.1	80 ± 9.2	43 ± 10.1
mPAP (mmHg)	NA	32 ± 10.8	68 ± 26.9	41 ± 6.8
pO_2 (mmHg)	NA	70 ± 12.1	70 ± 13.8	60 ± 20.4

Values are shown as mean ± SD.

Table 2. Demographics and clinical characteristics of COPD, IPAH, and PF patients and donors used for ELISA.

	Donor	COPD	IPAH	PF
Subjects (*N*)	35	24	15	10
Sex (male:female)	NA	8:16	4:11	7:3
Age at LTX (years)	NA			
BMI (kg/m^2)	NA	22.4 ± 3.2	23.7 ± 2.8	26.7 ± 3.7
Smoking status (never/former/active/unknown)	NA	2/22/1/0	NA	NA
FEV_1 (% predicted)	NA	23.7 ± 9.8	76.8 ± 10.1	45.9 ± 11.3
FVC (% predicted)	NA	50.3 ± 16.4	81.2 ± 12.9	38.4 ± 8.8
mPAP (mmHg)	NA	30.3 ± 9.7	56.2 ± 24.5	41.2 ± 9.3
pO_2 (mmHg)	NA	66.3 ± 11.7	46.2 ± 16.8	54.5 ± 16.2

Values are shown as mean ± SD.

informed consent was obtained from all subjects. The studies were approved by the Institutional Review Board of the Medical University of Graz (23-408 ex 10/11).

Hemodynamics from right heart catheterization was available for 28, 10, and 10 patients with COPD, IPAH, and idiopathic PF (IPF), respectively.

Plasma samples from patients with COPD ($n = 25$), IPAH ($n = 15$), and PF ($n = 10$) were collected prospectively from an IPAH cohort of patients who were treated at the Medical University of Graz (Graz, Austria) when undergoing diagnostic or follow-up right heart catheterization as well as from end-stage transplant patients (COPD, IPAH, and IPF) from the Department of Surgery, Division of Thoracic Surgery, Medical University of Vienna, Austria. Patient characteristics included age at LTX, BMI, sex, smoking status, oxygen requirement, pCO_2, pO_2, mPAP, and pulmonary function tests, and are presented in Table 3. The samples from the healthy controls ($n = 35$) were prospectively collected and stored in the Biobank of the Medical University of Graz between 2011 and 2014. Written informed consent was obtained from all subjects. The studies were approved by the Institutional Review Board of the Medical University of Graz (23-408 ex 10/11) as well as by the Institutional Review Board of the Medical University of Vienna (976/2010) in accordance with national law. Sample usage was approved by the institutional ethics committee and patient consent was obtained before LTX.

Table 3. Detailed clinical characteristics of COPD patients ($n = 28$) used for correlation analysis of ACE2 expression.

Parameter	Mean	SD	Minimum	Maximum
Age (years)	58	5.8	41	66.1
Height (cm)	168	8.1	150	182
Weight (kg)	63	9.6	50	90
BMI (kg/m^2)	22	3	18	29.1
Smoking status (pack-years)	45.2	24.6	0	120
6MWD (m)	211	133.4	0	424
FEV_1/FVC (%)	39	9.2	25.4	62
RV/TLC (%)	73	9.5	45.4	85.5
FEV_1 (% predicted)	23	10.9	9	63
FVC (% predicted)	49	17.4	24	88
TLC (% predicted)	140	25.4	65.8	186.1
RV (% predicted)	311	77.6	206	440.1
DLCOcSB (% predicted)	23	11.2	6.8	40.5
pO_2 (mmHg)	68	12.2	49	95.6
pCO_2 (mmHg)	51	11.9	34.4	79.9
CRP (mg/l)	1	2.4	0	9.7
RDW (%)	14	1.2	12.9	18
NTproBNP (pg/ml)	210	606.1	9.2	2,398
mPAP (mmHg)	32	9.9	16	62
Uric acid (mg/dl)	5	1.4	2.8	7.2
Bilirubin (mg/dl)	1	0.4	0.2	2
Serum albumin (mg/dl)	4	4	33.4	49.6

6MWD, 6-min walking distance; CRP, C-reactive protein; DLCOcSB, single breath diffusion capacity for carbon monoxide; NTproBNP, N-terminal brain natriuretic pro-peptide; RDW, red cell distribution width; RV, residual volume; TLC, total lung capacity.

Gene expression and protein analysis

Tissue samples were collected and cryopreserved in liquid nitrogen. Tissue was homogenized using mortar and pestle prior to RNA isolation. RNA was isolated using a peqGOLD Total RNA Kit (Peqlab, Erlangen, Germany). cDNA synthesis was performed using the qScript™ cDNA Synthesis Kit (Quantabio, Beverly, MA, USA) according to the manufacturer's instructions. Quantitative real-time PCR (qPCR) was performed using a LightCycler® 480 System (Roche Applied Science, Vienna, Austria). The qPCRs were set up using a QuantiFast® SYBR® Green PCR kit (Qiagen, Hilden, Germany) using the following protocol: 5 min at 95 °C (5 s at 95 °C, 5 s at 60 °C, and 10 s at 72 °C) × 45. The specificity of the reaction was confirmed based on melting curve analysis and gel electrophoresis. Primer sequences were as follows (5'→3'): *EZR*-fw GAGCACACGGAGCACTG, *EZR*-rv CCATGGTGGTAACTCGGACA; *ACE2*-fw CGAGTGGCTAATTTGAAACCAAGAA, *ACE2*-rv ATTGATACGGCTCCGGGACA; *TMPRSS2*-fw CAC GGACTGGATTTATCGACAA, *TMPRSS2*-rv CGTCAAGGACGAAGACCATGT; CD147/*BSG*-fw CTGTTCGTGCTGCTGGGATT, CD147/*BSG*-rv GGAGCCAAGGTCTTCTACGG; *FURIN*-fw GC AAAGCGACGGACTAAACG, *FURIN*-rv TGCC ATCGTCCAGAATGGAGA; *B2M*-fw CCTGGAGGC TATCCAGCGTACTCC, *B2M*-rv TGTC GGATGGATGAAACCCAGACA; and *HMBS*-fw ACCCTAGAAACCCTGCCAGAGAA, *HMBS*-rv GCCGGGTGTTGAGGTTTCCCC. *B2M* and PBGD/*HMBS* served as reference genes. The Δ*C*t values were calculated using the following formula: $\Delta Ct = Ct\,(\text{reference gene}) - Ct\,(\text{gene of interest})$. Δ*C*t values of donors and patients were normalized to the mean gene expression of donors (ΔΔ*C*t): $\Delta\Delta Ct = \Delta Ct\,\text{diseased} - \text{mean}\,\Delta Ct\,\text{of all donors}$.

A sandwich high-sensitivity enzyme-linked immunosorbent assay (ELISA) kit was used to quantitatively detect ACE2 (#SEB886Hu; Dianova GmbH, Hamburg, Germany) protein levels in plasma of COPD, IPAH, and PF patients and corresponding controls. The ELISA was performed according to the manufacturer's instructions and absorption values were measured on a ClarioStar microplate reader (BMG Labtech, Ortenberg, Germany).

Public dataset analysis

The microarray dataset GSE47460 using total RNA extracted from transplant lung homogenates was downloaded from GEO DataSets [24]. Expression values for each gene (*ACE2*, *TMPRSS2*, *FURIN*, *EZR*, and CD147/*BSG*) were extracted for the different disease states (COPD = 145, ILD = 193, CTRL = 91). In addition, the microarray datasets GSE8500 (COPD = 43, CTRL = 5; lung biopsy), GSE103174 (COPD = 44, CTRL = 21; lung explants), GSE37768 (COPD = 18, CTRL = 20; lung cancer resection), GSE110147 (IPF = 22, CTRL = 11; lung cancer resection), GSE53845 (IPF = 40, CTRL = 8; lung biopsy/explants), and GSE24988 (IPF-severe PH = 17, IPF-intermediate PH = 45, IPF-no PH = 22, validation set = 32; lung explants) were downloaded from GEO DataSets and analyzed for the respective gene set [25–29].

Single-cell RNA sequencing (scRNAseq) data from Adams *et al*'s study [30] were downloaded from GEO (GSE136831), and the Feature-Barcode Matrices were imported and analyzed in Seurat 3.1.1 [31]. As previously described, lung tissue samples were collected from explanted lungs and processed for scRNAseq after removal of visible airway structures, vessels, blood clots, and mucin [30]. Ten donor (003C, 065C, 137C, 160C, 244C, 253C, 296C, 454C, 465C, and 483C) and 10 COPD samples (052CO, 056CO, 178CO, 186CO, 194CO, 207CO, 237CO, 238CO, 23CO, and 8CO) were taken for further analysis; cells with high mitochondrial percentage > 10% were removed and data were normalized using default parameters. Dimension reduction was performed by Principal Component Analysis (PCA) and Uniform Manifold Approximation and Projection for Dimension Reduction (UMAP) using default parameters. Cells were clustered based on metadata as provided in Adams *et al*'s study [30]. To simplify readouts, the following clusters were manually concatenated to give dendritic cells (DC) (cDC1, cDC2, DC_Langerhans, DC_ Mature), Fibroblast (Fibroblast, Myofibroblast), innate lymphoid cells (ILC) (ILC_A, ILC_B), Monocyte (cMonocyte, ncMonocyte), T_cell (T, T_Cytotoxic, T_Regulatory), and Vascular_Endothelium (VE_Arterial, VE_Capillary_A, VE_Capillary_B, VE_Peribronchial, VE_Venous), all others retained original identity.

Histology

Formalin-fixed and paraffin-embedded lung tissue samples were cut into 2.5-µm thick serial sections for histological analysis. Sections were deparaffinized in ROTICLEAR® (Carl Roth, Arlesheim, Switzerland), followed by decreasing concentrations of ethanol. Antigen retrieval was performed using citrate buffer (pH 9) in a 95 °C hot water bath for 20 min. Following blocking with 3% BSA in PBS for 1 h, sections

were incubated with antibodies to ACE2 (1:100, #HPA000288; Sigma Aldrich, St Louis, MO, USA), TMPRSS2 (1:800, #bs-6285R; Biossusa, Woburn, MA, USA), Ezrin (1:100, #3145S; Cell Signaling Technology, Boston, MA, USA), Furin (1:100, #sc-133 142; Santa Cruz, Dallas, TX, USA), or CD147 (1:100, #AF972; R&D Systems, Minneapolis, MN, USA) at 4 °C overnight. The primary antibodies were detected with the immPRESS anti-rabbit, anti-goat, or anti-mouse polymer detection kit using NovaRed peroxidase (HRP) substrate (Vector Laboratories, Burlingame, CA, USA). Hemalaun was used for nuclear counterstaining. Images were obtained using an Olympus VS120 slide scanning microscope (Olympus, Tokyo, Japan) at ×40 magnification.

Statistics

Statistical analysis was performed in R (version number 4, www.r-project.org). Data are expressed as single data points with boxplot overlay indicating median and interquartile range. Multiple groups were compared using a nonparametric Kruskal–Wallis test. P values of <0.05 were considered as statistically significant.

Results

Local and systemic ACE2 levels in CLDs

We investigated a total of 49 explanted lungs and 10 donor lungs. While COPD and PF patients had major lung function limitation with a forced vital capacity (FVC) of 48 ± 18.1 and 43 ± 10.1, respectively, IPAH patients' lung function was more preserved (80 ± 9.2% predicted). As expected, IPAH patients had a severe increase of mPAP to 68 ± 27 mmHg. In COPD and PF, mPAP was elevated to 32 ± 11 mmHg in COPD and 41 ± 7) mmHg in PF patients. In all groups, hypoxemia was common with mean arterial pO_2 of 67 ± 12 mmHg in COPD, 70 ± 14 mmHg in IPAH, and 60 ± 20 mmHg in PF patients. General patient demographics and clinical characteristics are given in Table 1.

Despite differences regarding age and sex (Table 1), gene expression analysis of the SARS-CoV-2 receptor, *ACE2*, and interacting molecules showed a clear grouping within each patient cohort, indicating that expression of SARS-CoV-2-interacting molecules was highly group-dependent (Figure 1A). A striking increase of *ACE2* and *TMPRSS2* expression and a concomitant decrease of *FURIN* were detected in COPD patients compared to donor samples, while in IPAH and PF the expression levels were comparable to donor (Figure 1A). Similarly, *EZR* expression was highest in COPD compared to all other groups, but was also elevated in IPAH and PF compared to donor samples (Figure 1A). CD147/*BSG*, another suggested SARS-CoV-2 receptor, was significantly downregulated in COPD compared to donor, IPAH, and PF. ACE2 can be cleaved from the cell membrane and circulate in the plasma. As soluble ACE2 (sACE2) has been proposed to be beneficial in the fight against COVID-19 via neutralization of SARS-CoV-2 [32], we investigated sACE2 levels in the plasma of COPD, IPAH, and PF patients and healthy controls (Figure 1B). COPD and PF patients showed significantly decreased circulating sACE2 compared to healthy controls. In IPAH, sACE2 levels were unaltered and comparable to controls (Figure 1B). Patient's clinical characteristics are shown in Table 2.

To strengthen our investigations, we analyzed gene expression levels in publicly available microarray datasets of COPD lung tissue (GSE8500, GSE103174,

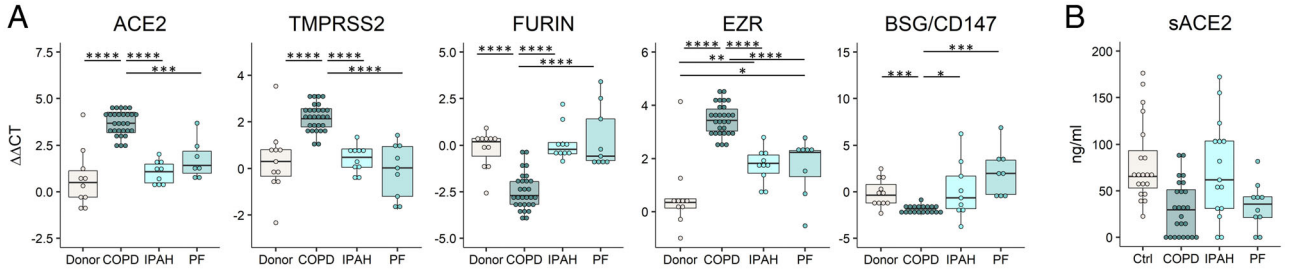

Figure 1. Local and systemic levels of SARS-CoV-2 receptors and processing enzymes in patients and controls. (A) Quantitative real-time PCR analysis of *ACE2*, *TMPRSS2*, Furin (*FURIN*), Ezrin (*EZR*), and CD147/Basigin (*BSG*) expression levels in lung homogenates of donors and transplant patients with COPD, IPAH, and PF. (B) sACE2 levels measured by ELISA in plasma samples of healthy controls (Ctrl), COPD, IPAH, and PF patients. Boxplots with single data points are shown. Statistical analysis was performed using a nonparametric Kruskal–Wallis test with *post hoc* comparison of multiple groups. *$p < 0.05$, **$p < 0.01$, ***$p < 0.001$, ****$p < 0.0001$.

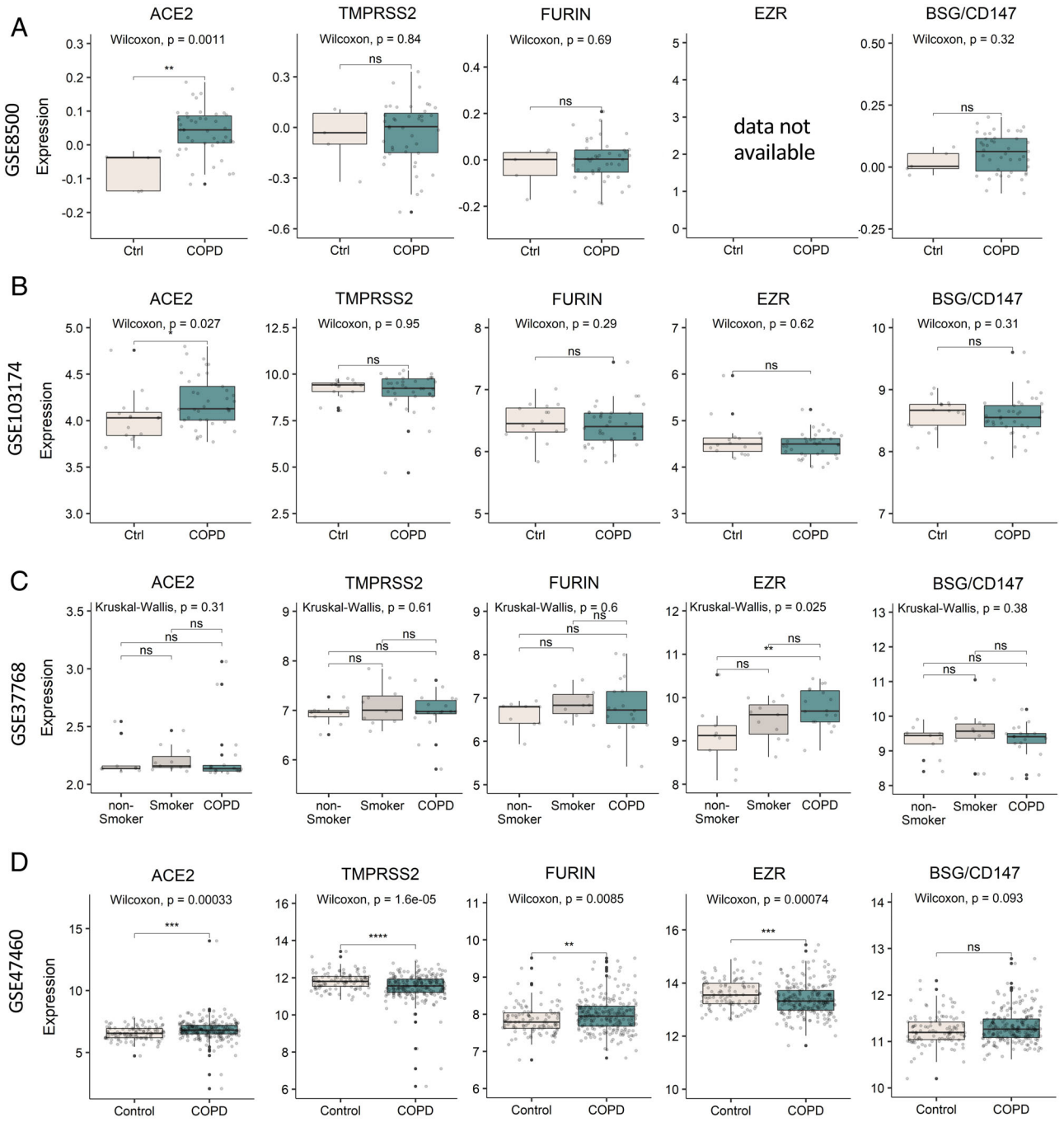

Figure 2. Expression profiling of SARS-CoV-2 receptors and processing enzymes in publicly available datasets of COPD and control lungs. Expression profiling in lung biopsy tissue (A, dataset GSE8500), lung explant tissue (B, D, datasets GSE103174 and GSE47460, respectively), and lung cancer resection tissue (C, dataset GSE37768) compared between COPD patients and donors. Boxplots with single data points are shown. Statistical analysis was performed using a nonparametric Kruskal–Wallis test with *post hoc* comparison of multiple groups. $^{*}p < 0.05$, $^{**}p < 0.01$, $^{***}p < 0.001$, $^{****}p < 0.0001$.

GSE37768, and GSE47460) and PF lung tissue (GSE110147, GSE53845, and GSE24988) compared to control lung tissue. In accordance with our data, *ACE2* expression was significantly elevated in COPD patients compared to control sample in three of the four analyzed COPD datasets, whereas *BSG* did not

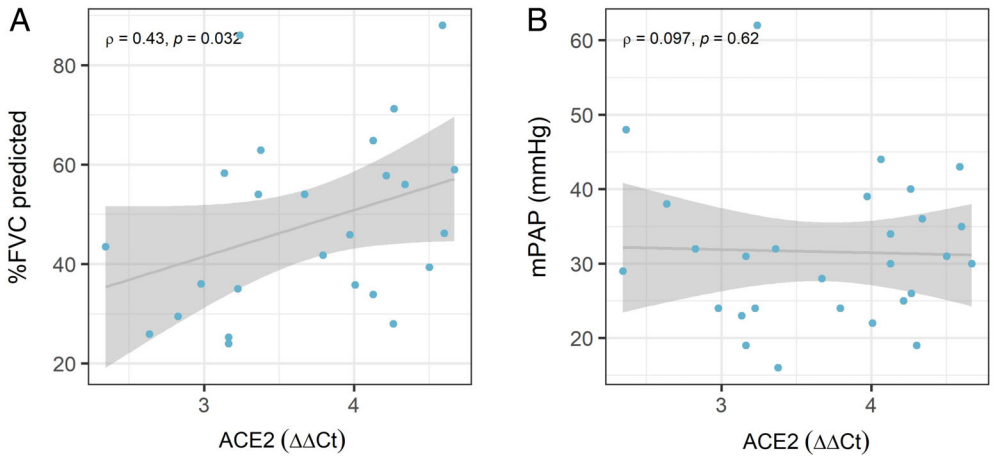

Figure 3. ACE2 expression in the lung correlates with lung function, but not with mPAP in COPD. Spearman's rank correlation of FVC (% predicted) (A) or mPAP (mmHg) (B) with *ACE2* expression levels ($\Delta\Delta Ct$).

show any significant changes between COPD patients and donors (Figure 2). Minor differences in the expression of *TMPRSS2*, *FURIN*, and *EZR* were inconsistent across different COPD cohorts (Figure 2). Furthermore, the comparison of gene expression levels between nonsmokers, smokers, and COPD patients (GSE37768) did not show any significant expression differences, except for *EZR* (Figure 2C).

By comparing expression levels between IPF patients and donors, we did not reveal consistent changes across the analyzed datasets GSE110147 and GSE53845 (see supplementary material, Figure S1A, B); however, significant gene expression regulation was observable for all analyzed genes. ACE2 expression was found to be opposite in the two datasets. Different types of control (donor transplant tissue versus cancer resection tissue) and IPF lung tissue from different disease stages (biopsy versus lung transplant) as well as region of sampling could represent key parameters for this contrary gene expression result. Importantly, no significant changes in gene expression levels were observed when different stages of PH were compared in PF patients (see supplementary material, Figure S1C).

Due to the strong expression changes of *ACE2* and *TMPRSS2* observed in our COPD cohort and the consistent changes of *ACE2* expression in the analyzed datasets, we decided to focus further investigations on this disease.

ACE2 correlations with clinical characteristics

ACE2 expression levels showed a significant positive correlation with FVC in COPD patients ($\rho = 0.43$, $p = 0.032$; Figure 3A). However, correlations with hemodynamic parameters, such as mPAP, were not significant (Figure 3B). Detailed characteristics of lung function, hemodynamic, and clinical parameters of patients are shown in Table 3.

Cellular sources and localization

As SARS-CoV-2 receptor ACE2 and diverse proteases facilitating virus entry have to be in very close proximity or on the same target cell to allow viral entry, we investigated a publicly available scRNAseq dataset from Adams *et al*'s study [30] (GSE136831) for cell type-specific expression levels in control samples and COPD patients (Figure 4A). *ACE2* expression was mostly below the detection limit in control and COPD samples, indicating low expression levels which were not captured by the depth provided by the 10X Genomics (Pleasanton, CA, USA) platform; therefore, more sensitive analytical methods are required. Nevertheless, other genes investigated by scRNAseq were sufficiently captured and analyzed: *TMPRSS2* expression was observed almost exclusively in epithelial cells of the lung, such as alveolar type (AT) II cells, ATI, and club cells (Figure 4B,C). *FURIN* was expressed ubiquitously (also in epithelial cells) with the strongest signal in macrophages and monocytes in both COPD and control lungs (Figure 4C). *EZR* was expressed by most cell types but the average expression was most prominent in epithelial cells (ATI, ATII, goblet, club, and ciliated cells) and in inflammatory cell subsets (e.g. dendritic cells and monocytes) (Figure 4C).

We next substantiated these findings at the protein level using immunohistochemistry. ACE2 immunoreactivity

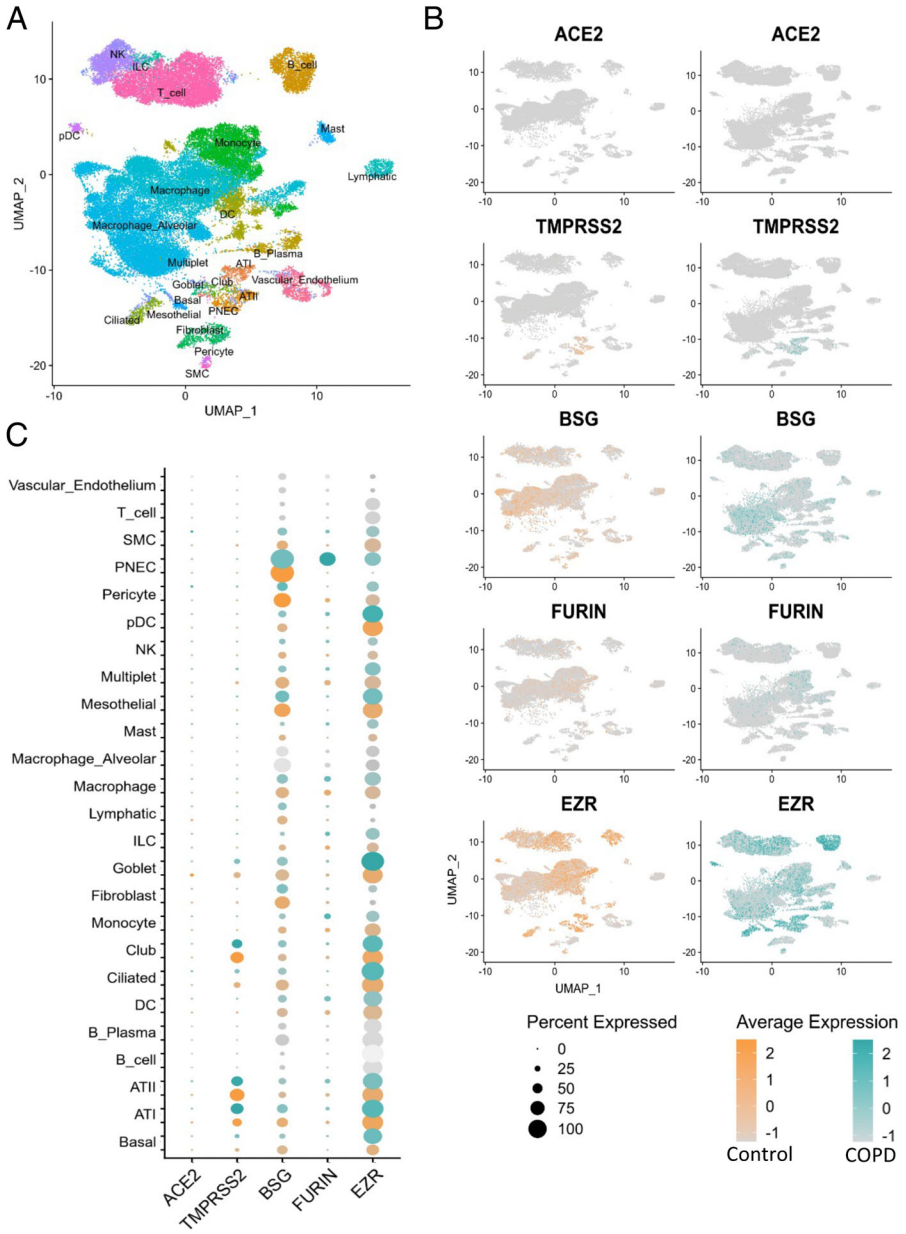

Figure 4. scRNAseq reveals cell type-specific expression of SARS-CoV-2 receptors and processing enzymes in COPD and control lungs. (A) Uniform Manifold Approximation and Projection for Dimension Reduction (UMAP) representation of cell clusters in control and COPD lungs. Dots represent single cells. ATI, alveolar type I cells; ATII, alveolar type II cells; B_Plasma, plasma cells; DC, dendritic cells; ILC, innate lymphoid cells; Lymphatic, lymphatic endothelium; Mast, mast cells; NK, natural killer cells; pDC, plasmacytoid dendritic cells; PNEC, pulmonary neuroendocrine cell; SMC, smooth muscle cell. (B) Expression of *ACE2*, *TMPRSS2*, *BSG* (CD147), *FURIN*, and *EZR* in single cells of control and COPD lungs. Cell clusters are shown as indicated in (A). (C) Dot plot representation of *ACE2*, *TMPRSS2*, *BSG* (CD147), *FURIN*, and *EZR* expression in specific cell populations within control and COPD lungs. Dot sizes represent the percent of cells within each cluster with positive gene expression and color intensity indicates the average expression of within one cluster.

was present in epithelial cells with the most prominent staining in bronchial and alveolar epithelial cells in COPD lungs (see supplementary material, Figure S2). Detailed analysis of ACE2, TMPRSS2, Furin, Ezrin, and CD147 localization was performed on corresponding serial sections (Figure 5). In healthy donor tissue, ACE2 almost exclusively localized to the bronchial epithelial layer (black arrowheads) with light

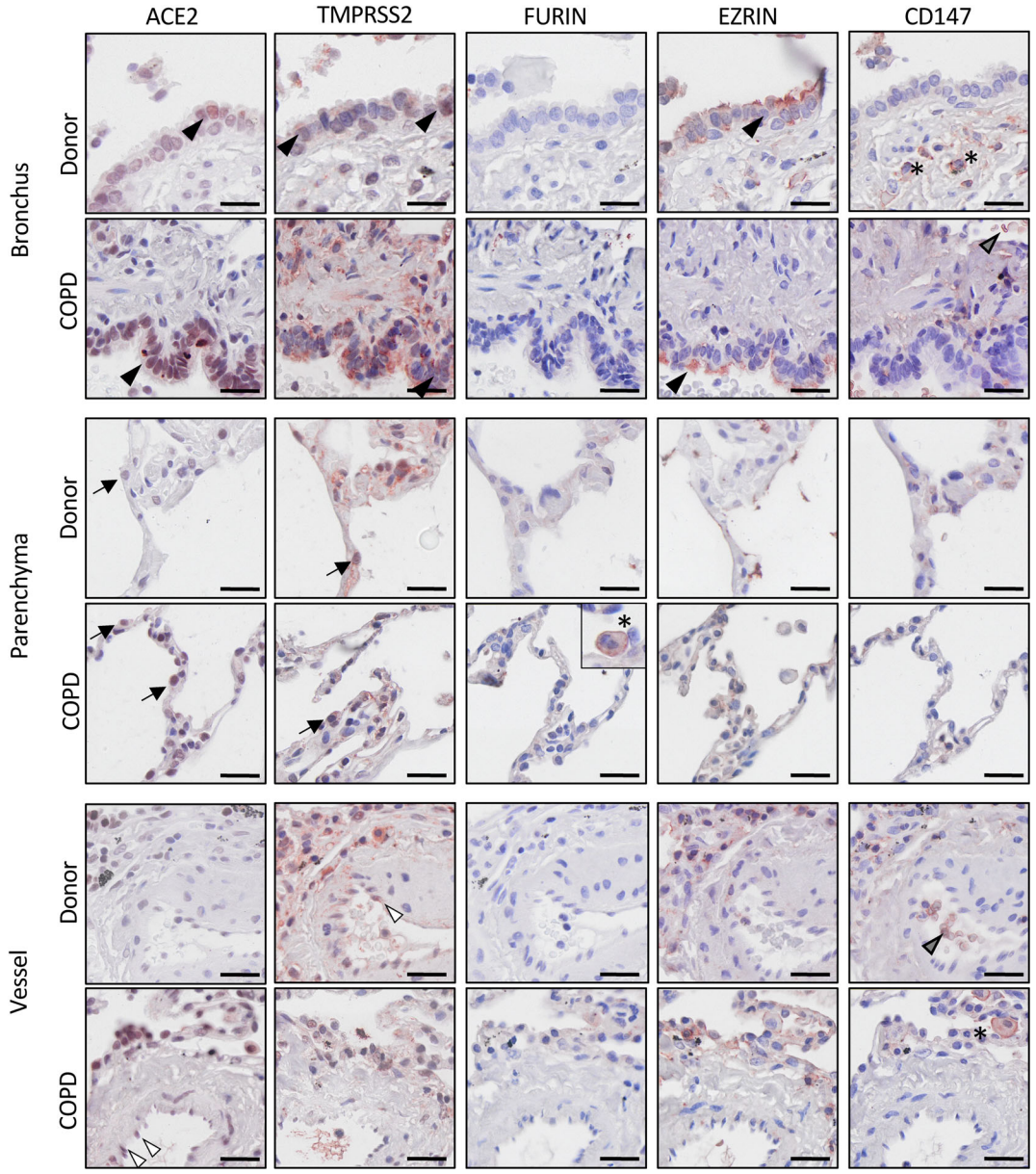

Figure 5. Immunostaining reveals cellular localization of SARS-CoV-2 receptors and processing enzymes in COPD and donor lung tissue. High-magnification images showing ACE2, TMPRSS2, Furin, Ezrin, and CD147 immunostaining in bronchial, parenchymal, and vascular compartments on corresponding serial sections of donor and COPD tissue. Scalebar = 20 µm. Black arrowhead, bronchial epithelium; black arrow, alveolar epithelial type II cells; white arrowhead, vascular endothelium; gray arrowhead, erythrocytes; asterisks, inflammatory cells.

staining in ATII cells (black arrows), but no detectable staining in the vascular compartment. In COPD, a clear signal was visible in bronchial and ATII cells, as well as very weak staining in vascular endothelial cells (white arrowhead) which was in contrast to healthy donor tissue. Immunoreactivity against TMPRSS2 was observed ubiquitously in bronchial, parenchymal, and vascular regions in both donor and COPD lungs (Figure 5). Similar to our scRNAseq analysis, very few cells stained positive for Furin, and immunoreactivity was almost undetectable in structural cells, while monocytes and macrophages showed clear immunoreactivity (Figure 5, parenchymal panel, inset). Ezrin was localized to the bronchial epithelium and in

perivascular regions. CD147 localized mostly to inflammatory cells, such as macrophages (asterisks), and on the surface of erythrocytes (gray arrowheads). In the airway epithelium and submucosal cells, CD147 was partially observable. Cumulatively, our data point toward predominant expression of ACE2 and TMPRSS2 in bronchial as well as alveolar epithelial cells in COPD lungs.

Discussion

Although knowledge about SARS-CoV-2 and related COVID-19 is growing, there are limited data on the expression of genes interacting with the virus and their effects on disease susceptibility and severity in CLD patients. In addition to binding to its main receptor ACE2 [5,6], SARS-CoV-2 entry additionally depends on the proteases Furin and TMPRSS2 and cofactor EZR [5,33–35]. Besides ACE2, CD147 (*BSG*) has been proposed as a possible SARS-CoV-2-binding receptor in endothelial cells, but with contradictory and inconclusive results [9,10]. In line with published data, we did not observe any detectable expression of CD147 protein in vascular or microvascular endothelium [9]. RNA expression levels were unaltered in IPAH and PF and decreased in COPD, indicating that altered CD147 expression may not explain any potential increase of SARS-CoV-2 infection risk in patients with CLDs. Furthermore, Neuropilin-1 (NRP1) has been debated as a putative host factor, interacting with SARS-CoV-2 [36,37]. However, we did not observe any regulation of NRP1 in any of the investigated diseases in our cohorts or publicly available datasets (data not shown).

Several studies have used publicly available scRNAseq datasets to investigate SARS-CoV-2 virulence gene expression in healthy and diseased tissue. One common factor of all used datasets and also observed in this study is very limited detection of the main virus receptor ACE2 in scRNAseq datasets [38,39]. While use of such datasets may have a huge potential for more abundant genes, detection of ACE2 is limited by the method's depth. To understand the actual viral interactions possibly occurring in the lungs of CLD patients, more sensitive methods, such as qPCR or analysis of protein levels, as performed in our study, are required. Using these methods, we observed a striking increase of ACE2 in COPD, as was also observed recently by other research groups [40,41]. As viral infections are particularly relevant in this disease, where they can lead to systemic inflammation and recurrent exacerbations with slow recovery of symptoms [42], it is highly relevant to further investigate new susceptibility factors to SARS-CoV-2 infections in COPD patients.

COPD appears to be underrepresented in the comorbidities reported for patients infected with COVID-19 [40,43], although several studies show an increased risk for a severe COVID-19 infection and increased mortality in patients with COPD [2,40,44]. Recent meta-analyses of early COVID-19 cohorts and more robust COVID-19 registry data from bigger centers [45–47] confirm that, although the infection rates do not differ between COPD and non-COPD, the risk of severe COVID-19 is increased in COPD, as indicated by increased hospitalization rates, ICU admission, and need for mechanical ventilation [45–47]. Interpretation of such studies is difficult because the general health status and comorbidities of COPD patients may be strongly associated with the outcome of SARS-COV-2 infection [48,49].

It has been suggested that increased COVID-19 mortality might be due to increased levels of *ACE2* expression in the smaller airways of COPD patients and smokers [41]. Increased ACE2 expression was supported by our analysis, where a marked increase was found in various publicly available datasets of different COPD patient cohorts. In our explanted lung tissue, we could expand on these findings and show that not only *ACE2* levels, but also TMPRSS2 and EZR are elevated in the lung tissue of COPD patients compared to control donor samples. Moreover, we could show increased ACE2 and TMPRSS2 expression levels not only in airway epithelial cells, but also in the lung parenchyma, including alveolar epithelial cells. While Leung *et al* [41] reported an inverse correlation of ACE2 levels with forced expiratory volume in 1 s (FEV_1) % predicted, our data indicated a positive correlation. This discrepancy might be due to the fact that Leung *et al* used ACE2 protein levels of small airway epithelium only, while we investigated *ACE2* expression in the whole lung tissue.

The importance of the renin–angiotensin–aldosterone system (RAAS) in the pathophysiology of various pulmonary diseases has been established in recent years [50–55]. In COPD, a dysbalance of vasoactive components of the RAAS has been postulated and therapeutically shifting the balance toward ACE2 provides beneficial effects in the patients [55,56]. By binding angiotensin II, a key regulatory component of the RAAS, ACE2 acts in a vasodilative and anti-inflammatory manner, counterbalancing the proinflammatory, vasoconstrictive, and profibrotic ACE-angiotensin I axis [7]. The exact role of the ACE2-angiotensin II axis in the pathogenesis of

COPD however remains unexplored. While an increase in pulmonary ACE2 might be a protective mechanism in response to the COPD-associated changes [57], it could contribute to a worse COVID-19 outcome. Increased availability of SARS-CoV-2-susceptible cells expressing ACE2 together with TMPRSS2 and Ezrin in the distal bronchioles and lung parenchyma of COPD patients could facilitate more efficient entry and spread of SARS-CoV-2 viral particles within the distal parts of the lung, leading to severe disease progression. Therefore, administration of inhaled corticosteroids, an immunomodulatory medication, is currently being investigated to reduce disease susceptibility and mortality by downregulating ACE2 expression in COPD patients [58,59].

In addition, ACE2 can be released from the cell surface via proteases, including Adam17 and Adam10 [60,61]. The soluble ectodomain of ACE2 (sACE2) maintains systemic protective effects and further binds and neutralizes SARS-CoV-2, thereby limiting virus propagation [60,62]. The significant decrease of circulating sACE2 in COPD patients might therefore negatively influence disease outcome. The possible application of recombinant sACE2 is currently under investigation [32,63,64]. Taken together, our data showing increased local expression and decreased circulating levels of sACE2 could explain an elevated risk of severe COVID-19 pneumonia in COPD patients.

ACE2 expression did not correlate with mPAP or other hemodynamic parameters in COPD patients, indicating that the presence of PH *per se* might not be a risk factor for severe COVID-19. The analysis of a publicly available dataset of IPF patients with different degrees of PH did not show differences in the expression of any of the genes in our set between different PH levels. Recently, Sandoval *et al* investigated the ACE2-Ang(1–7) axis in human PAH and found increased serum ACE2 levels with a concomitant loss of ACE2 activity compared to healthy controls, suggesting a dysregulated RAAS in these patients [65]. However, in our IPAH patient group both locally in the lung or systemically in the plasma, we could not observe differences in expression levels regarding genes relevant for SARS-CoV-2 susceptibility and plasma ACE2 levels as compared to healthy controls.

In conclusion, our data offer a potential explanation for the increased risk of worse COVID-19 outcome in COPD patients, through increased expression levels of SARS-CoV-2 relevant genes *ACE2* and *TMPRSS2* in the distal lung with a concomitant decline of protective sACE2 levels in the circulation, independent of the presence or absence of PH.

Acknowledgements

We would like to thank Elisabeth Blanz and Thomas Fuchs for excellent technical assistance. PhD candidate EF was funded by the Austrian Research Promotion Agency (FFG, project number: 34926649) and trained within the frame of the PhD program Molecular Medicine of the Medical University of Graz. LMM is supported by FWF grant (KLI 884-B).

Author contributions statement

EF, AB and GK contributed to the conception and design of the study. EF, AB, EG and WK were responsible for sample and data acquisition. LMM performed scRNAseq analysis. EF, AB, LMM, HO and GK were involved in data analysis and interpretation. EF and AB drafted the first manuscript and all authors critically revised the manuscript.

References

1. Huang C, Wang Y, Li X, *et al*. Clinical features of patients infected with 2019 novel coronavirus in Wuhan, China. *Lancet* 2020; **395:** 497–506.
2. Lippi G, Henry BM. Chronic obstructive pulmonary disease is associated with severe coronavirus disease 2019 (COVID-19). *Respir Med* 2020; **167:** 105941.
3. Wang B, Li R, Lu Z, *et al*. Does comorbidity increase the risk of patients with COVID-19: evidence from meta-analysis. *Aging (Albany NY)* 2020; **12:** 6049–6057.
4. Zhao Q, Meng M, Kumar R, *et al*. The impact of COPD and smoking history on the severity of COVID-19: a systemic review and meta-analysis. *J Med Virol* 2020; **92:** 1915–1921.
5. Hoffmann M, Kleine-Weber H, Schroeder S, *et al*. SARS-CoV-2 cell entry depends on ACE2 and TMPRSS2 and is blocked by a clinically proven protease inhibitor. *Cell* 2020; **181:** 271–280.e8.
6. Li W, Moore MJ, Vasilieva N, *et al*. Angiotensin-converting enzyme 2 is a functional receptor for the SARS coronavirus. *Nature* 2003; **426:** 450–454.
7. Jia H. Pulmonary angiotensin-converting enzyme 2 (ACE2) and inflammatory lung disease. *Shock* 2016; **46:** 239–248.
8. Hamming I, Timens W, Bulthuis ML, *et al*. Tissue distribution of ACE2 protein, the functional receptor for SARS coronavirus. A first step in understanding SARS pathogenesis. *J Pathol* 2004; **203:** 631–637.
9. Shilts J, Wright GJ. No evidence for basigin/CD147 as a direct SARS-CoV-2 spike binding receptor. *Sci Rep* 2021; **11:** 413.
10. Acosta Saltos F, Acosta Saltos AD. Entry of SARS-CoV2 through the basal surface of alveolar endothelial cells – a proposed mechanism mediated by CD147 in COVID-19. *Preprints* 2020; 2020050359 [Not peer reviewed].

11. Walls AC, Park YJ, Tortorici MA, *et al*. Structure, function, and antigenicity of the SARS-CoV-2 spike glycoprotein. *Cell* 2020; **183:** 1735.
12. Lai CC, Shih TP, Ko WC, *et al*. Severe acute respiratory syndrome coronavirus 2 (SARS-CoV-2) and coronavirus disease-2019 (COVID-19): the epidemic and the challenges. *Int J Antimicrob Agents* 2020; **55:** 105924.
13. Varga Z, Flammer AJ, Steiger P, *et al*. Endothelial cell infection and endotheliitis in COVID-19. *Lancet* 2020; **395:** 1417–1418.
14. Maremanda KP, Sundar IK, Li D, *et al*. Age-dependent assessment of genes involved in cellular senescence, telomere, and mitochondrial pathways in human lung tissue of smokers, COPD, and IPF: associations with SARS-CoV-2 COVID-19 ACE2-TMPRSS2-Furin-DPP4 Axis. *Front Pharmacol* 2020; **11:** 584637.
15. Radzikowska U, Ding M, Tan G, *et al*. Distribution of ACE2, CD147, CD26, and other SARS-CoV-2 associated molecules in tissues and immune cells in health and in asthma, COPD, obesity, hypertension, and COVID-19 risk factors. *Allergy* 2020; **75:** 2829–2845.
16. Jackson DJ, Busse WW, Bacharier LB, *et al*. Association of respiratory allergy, asthma, and expression of the SARS-CoV-2 receptor ACE2. *J Allergy Clin Immunol* 2020; **146:** 203–206.e3.
17. Choi YJ, Park JY, Lee HS, *et al*. Effect of asthma and asthma medication on the prognosis of patients with COVID-19. *Eur Respir J* 2021; **57:** 2002226.
18. Broadhurst R, Peterson R, Wisnivesky JP, *et al*. Asthma in COVID-19 hospitalizations: an overestimated risk factor? *Ann Am Thorac Soc* 2020; **17:** 1645–1648.
19. Belge C, Quarck R, Godinas L, *et al*. COVID-19 in pulmonary arterial hypertension and chronic thromboembolic pulmonary hypertension: a reference centre survey. *ERJ Open Res* 2020; **6:** 00520-2020.
20. Horn EM, Chakinala M, Oudiz R, *et al*. Could pulmonary arterial hypertension patients be at a lower risk from severe COVID-19? *Pulm Circ* 2020; **10:** 2045894020922799.
21. Nagaraj C, Tabeling C, Nagy BM, *et al*. Hypoxic vascular response and ventilation/perfusion matching in end-stage COPD may depend on p22phox. *Eur Respir J* 2017; **50:** 1601651.
22. Hoffmann J, Wilhelm J, Marsh LM, *et al*. Distinct differences in gene expression patterns in pulmonary arteries of patients with chronic obstructive pulmonary disease and idiopathic pulmonary fibrosis with pulmonary hypertension. *Am J Respir Crit Care Med* 2014; **190:** 98–111.
23. Hoffmann J, Marsh LM, Pieper M, *et al*. Compartment-specific expression of collagens and their processing enzymes in intrapulmonary arteries of IPAH patients. *Am J Physiol Lung Cell Mol Physiol* 2015; **308:** L1002–L1013.
24. Kim S, Herazo-Maya JD, Kang DD, *et al*. Integrative phenotyping framework (iPF): integrative clustering of multiple omics data identifies novel lung disease subphenotypes. *BMC Genomics* 2015; **16:** 924.
25. Wang IM, Stepaniants S, Boie Y, *et al*. Gene expression profiling in patients with chronic obstructive pulmonary disease and lung cancer. *Am J Respir Crit Care Med* 2008; **177:** 402–411.
26. Cruz T, López-Giraldo A, Noell G, *et al*. Multi-level immune response network in mild-moderate chronic obstructive pulmonary disease (COPD). *Respir Res* 2019; **20:** 152.
27. Cecchini MJ, Hosein K, Howlett CJ, *et al*. Comprehensive gene expression profiling identifies distinct and overlapping transcriptional profiles in non-specific interstitial pneumonia and idiopathic pulmonary fibrosis. *Respir Res* 2018; **19:** 153.
28. DePianto DJ, Chandriani S, Abbas AR, *et al*. Heterogeneous gene expression signatures correspond to distinct lung pathologies and biomarkers of disease severity in idiopathic pulmonary fibrosis. *Thorax* 2015; **70:** 48–56.
29. Mura M, Anraku M, Yun Z, *et al*. Gene expression profiling in the lungs of patients with pulmonary hypertension associated with pulmonary fibrosis. *Chest* 2012; **141:** 661–673.
30. Adams TS, Schupp JC, Poli S, *et al*. Single-cell RNA-seq reveals ectopic and aberrant lung-resident cell populations in idiopathic pulmonary fibrosis. *Sci Adv* 2020; **6:** eaba1983.
31. Stuart T, Butler A, Hoffman P, *et al*. Comprehensive integration of single-cell data. *Cell* 2019; **177:** 1888–1902.e21.
32. Zoufaly A, Poglitsch M, Aberle JH, *et al*. Human recombinant soluble ACE2 in severe COVID-19. *Lancet Respir Med* 2020; **8:** 1154–1158.
33. Hoffmann M, Kleine-Weber H, Pöhlmann S. A multibasic cleavage site in the spike protein of SARS-CoV-2 is essential for infection of human lung cells. *Mol Cell* 2020; **78:** 779–784.e5.
34. Millet JK, Kien F, Cheung CY, *et al*. Ezrin interacts with the SARS coronavirus spike protein and restrains infection at the entry stage. *PLoS One* 2012; **7:** e49566.
35. Vankadari N, Wilce JA. Emerging WuHan (COVID-19) coronavirus: glycan shield and structure prediction of spike glycoprotein and its interaction with human CD26. *Emerg Microbes Infect* 2020; **9:** 601–604.
36. Cantuti-Castelvetri L, Ojha R, Pedro LD, *et al*. Neuropilin-1 facilitates SARS-CoV-2 cell entry and infectivity. *Science* 2020; **370:** 856–860.
37. Davies J, Randeva HS, Chatha K, *et al*. Neuropilin1 as a new potential SARSCoV2 infection mediator implicated in the neurologic features and central nervous system involvement of COVID19. *Mol Med Rep* 2020; **22:** 4221–4226.
38. Zhang Q, Yue Y, Tan H, *et al*. Single cell RNA-seq data analysis reveals the potential risk of SARS-CoV-2 infection among different respiratory system conditions. *Front Genet* 2020; **11:** 942.
39. Singh M, Bansal V, Feschotte C. A single-cell RNA expression map of human coronavirus entry factors. *Cell Rep* 2020; **32:** 108175.
40. Jacobs M, Van Eeckhoutte HP, Wijnant SRA, *et al*. Increased expression of ACE2, the SARS-CoV-2 entry receptor, in alveolar and bronchial epithelium of smokers and COPD subjects. *Eur Respir J* 2020; **56:** 2002378.
41. Leung JM, Yang CX, Tam A, *et al*. ACE-2 expression in the small airway epithelia of smokers and COPD patients: implications for COVID-19. *Eur Respir J* 2020; **55:** 2000688.
42. George SN, Garcha DS, Mackay AJ, *et al*. Human rhinovirus infection during naturally occurring COPD exacerbations. *Eur Respir J* 2014; **44:** 87–96.
43. Halpin DMG, Faner R, Sibila O, *et al*. Do chronic respiratory diseases or their treatment affect the risk of SARS-CoV-2 infection? *Lancet Respir Med* 2020; **8:** 436–438.
44. Pranata R, Soeroto AY, Huang I, *et al*. Effect of chronic obstructive pulmonary disease and smoking on the outcome of COVID-19. *Int J Tuberc Lung Dis* 2020; **24:** 838–843.

45. Leung JM, Niikura M, Yang CWT, *et al*. COVID-19 and COPD. *Eur Respir J* 2020; **56:** 2002108.
46. Attaway AA, Zein J, Hatipoğlu US. SARS-CoV-2 infection in the COPD population is associated with increased healthcare utilization: an analysis of Cleveland clinic's COVID-19 registry. *EClinicalMedicine* 2020; **26:** 100515.
47. Guan WJ, Liang WH, Zhao Y, *et al*. Comorbidity and its impact on 1590 patients with COVID-19 in China: a nationwide analysis. *Eur Respir J* 2020; **55:** 2000547.
48. Trinkmann F, Saur J, Borggrefe M, *et al*. Cardiovascular comorbidities in chronic obstructive pulmonary disease (COPD) – current considerations for clinical practice. *J Clin Med* 2019; **8:** 69.
49. Huiart L, Ernst P, Suissa S. Cardiovascular morbidity and mortality in COPD. *Chest* 2005; **128:** 2640–2646.
50. de Man FS, Tu L, Handoko ML, *et al*. Dysregulated renin-angiotensin-aldosterone system contributes to pulmonary arterial hypertension. *Am J Respir Crit Care Med* 2012; **186:** 780–789.
51. Hemnes AR, Rathinasabapathy A, Austin EA, *et al*. A potential therapeutic role for angiotensin-converting enzyme 2 in human pulmonary arterial hypertension. *Eur Respir J* 2018; **51:** 1702638.
52. Wang J, Chen L, Chen B, *et al*. Chronic activation of the renin-angiotensin system induces lung fibrosis. *Sci Rep* 2015; **5:** 15561.
53. Marshall RP, Gohlke P, Chambers RC, *et al*. Angiotensin II and the fibroproliferative response to acute lung injury. *Am J Physiol Lung Cell Mol Physiol* 2004; **286:** L156–L164.
54. Curtis KJ, Meyrick VM, Mehta B, *et al*. Angiotensin-converting enzyme inhibition as an adjunct to pulmonary rehabilitation in chronic obstructive pulmonary disease. *Am J Respir Crit Care Med* 2016; **194:** 1349–1357.
55. Kim J, Lee JK, Heo EY, *et al*. The association of renin-angiotensin system blockades and pneumonia requiring admission in patients with COPD. *Int J Chron Obstruct Pulmon Dis* 2016; **11:** 2159–2166.
56. Tan WSD, Liao W, Zhou S, *et al*. Targeting the renin-angiotensin system as novel therapeutic strategy for pulmonary diseases. *Curr Opin Pharmacol* 2018; **40:** 9–17.
57. Xue T, Wei N, Xin Z, *et al*. Angiotensin-converting enzyme-2 overexpression attenuates inflammation in rat model of chronic obstructive pulmonary disease. *Inhal Toxicol* 2014; **26:** 14–22.
58. Finney LJ, Glanville N, Farne H, *et al*. Inhaled corticosteroids downregulate the SARS-CoV-2 receptor ACE2 in COPD through suppression of type I interferon. *J Allergy Clin Immunol* 2021; **147:** 510–519.e5.
59. Schultze A, Walker AJ, MacKenna B, *et al*. Risk of COVID-19-related death among patients with chronic obstructive pulmonary disease or asthma prescribed inhaled corticosteroids: an observational cohort study using the OpenSAFELY platform. *Lancet Respir Med* 2020; **8:** 1106–1120.
60. Jia HP, Look DC, Tan P, *et al*. Ectodomain shedding of angiotensin converting enzyme 2 in human airway epithelia. *Am J Physiol Lung Cell Mol Physiol* 2009; **297:** L84–L96.
61. Lambert DW, Yarski M, Warner FJ, *et al*. Tumor necrosis factor-alpha convertase (ADAM17) mediates regulated ectodomain shedding of the severe-acute respiratory syndrome-coronavirus (SARS-CoV) receptor, angiotensin-converting enzyme-2 (ACE2). *J Biol Chem* 2005; **280:** 30113–30119.
62. Monteil V, Kwon H, Prado P, *et al*. Inhibition of SARS-CoV-2 infections in engineered human tissues using clinical-grade soluble human ACE2. *Cell* 2020; **181:** 905–913.e7.
63. Alhenc-Gelas F, Drueke TB. Blockade of SARS-CoV-2 infection by recombinant soluble ACE2. *Kidney Int* 2020; **97:** 1091–1093.
64. Abd El-Aziz TM, Al-Sabi A, Stockand JD. Human recombinant soluble ACE2 (hrsACE2) shows promise for treating severe COVID-19. *Signal Transduct Target Ther* 2020; **5:** 258.
65. Sandoval J, Del Valle-Mondragón L, Masso F, *et al*. Angiotensin converting enzyme 2 and angiotensin (1-7) axis in pulmonary arterial hypertension. *Eur Respir J* 2020; **56:** 1902416.

SUPPLEMENTARY MATERIAL ONLINE

Figure S1. Expression profiling of SARS-CoV-2 receptors and processing enzymes in publicly available datasets of IPF and control lungs

Figure S2. Immunostaining indicating tissue distribution of SARS-CoV-2 receptor ACE2 in COPD and donor lung tissue